

**NANO EXPRESS**

**Open Access**

# The magnetic-nanofluid heat pipe with superior thermal properties through magnetic enhancement

Yuan-Ching Chiang<sup>1</sup>, Jen-Jie Chieh<sup>2\*</sup> and Chia-Che Ho<sup>3</sup>

## Abstract

This study developed a magnetic-nanofluid (MNF) heat pipe (MNFHP) with magnetically enhanced thermal properties. Its main characteristic was additional porous iron nozzle in the evaporator and the condenser to form a unique flowing pattern of MNF slug and vapor, and to magnetically shield the magnet attraction on MNF flowing. The results showed that an optimal thermal conductivity exists in the applied field of 200 Oe. Furthermore, the minor thermal performance of MNF at the condenser limited the thermal conductivity of the entire MNFHP, which was 1.6 times greater than that filled with water for the input power of 60 W. The feasibilities of an MNFHP with the magnetically enhanced heat transfer and the ability of vertical operation were proved for both a promising heat-dissipation device and the energy architecture integrated with an additional energy system.

**Keywords:** Magnetic nanofluids, Thermal conductivity, Slug, Vapor

## Background

With the gradually increasing development of dense electrical circuit electronics, several aspects were considered for the typical improvements on a heat pipe, referred to as a heat superconductor. Nanofluids with excellent thermal conductivity [1] were applied as the working fluids (WFs) of traditional heat pipes to enhance the thermal performance [2,3]. However, either high-cost metal nanoparticles solved in water were used as nanofluids or these heat pipes were operated only in a horizontal or limited tilt arrangement, rather than the vertical arrangement, in which their thermal performance deteriorates because nanoparticles always accumulate on the evaporator of heat pipes with evaporation converting water to vapor.

An oscillating heat pipe [4-6] with an additional heat transfer mechanism of conventional force through the interval liquid slug and vapor bubble beyond that of the phase change can overcome the deposition problem. Its closed loop suppresses the entrainment limit, that is, the

shear force between condensing and evaporating flow in high-input power [7]. However, its multi-turn architecture limits its integration with electronics.

Among low-cost metal-oxide nanofluids [8-10], magnetic nanofluids (MNFs) have the magnetically enhanced thermal conductivity [8,9] to compete with metal nanofluids. However, the common disadvantage of developed MNFHPs in overcoming the deposition problems is the extra-induced problem of magnetic manipulation resulting from unsuitable designs of either active or complex magnetic fields [11,12]. To avoid the extra power consumption from actively controlling the MNF flowing, a novel MNFHP in a closed-loop architecture was proposed for several main objects: the first was the flowing pattern of the interval vapor moving the MNF slug; the second was the superior suppression of the entrainment limit; and the third was the expansible ability for the integration with some energy storage [13].

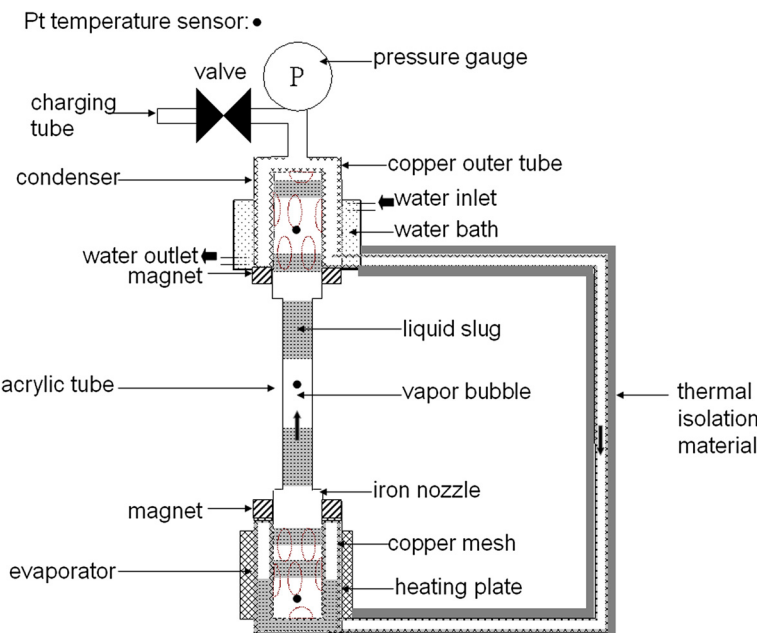
## Methods

Figure 1 shows a closed-loop type of MNFHP. Its main difference from traditional heat pipes is the inner structure, that is, the additional iron porous nozzle in both evaporator and condenser, and magnets on its evaporator and condenser. The iron porous nozzle suppresses

\* Correspondence: jjchieh@ntnu.edu.tw

<sup>2</sup>Institute of Electro-Optical Science and Technology, National Taiwan Normal University, No.88, Sec.4, Ting-Chou Rd., Taipei 116, Taiwan

Full list of author information is available at the end of the article



**Figure 1** The closed-loop type of a MNFHP.

magnetic attraction for MNF flowing and forms the flowing pattern of the interval flowing of MNF slug and vapor bubble. Similarly, copper meshes sintered on whole inner surface were also used to transport MNFs by the capillary force against the magnetic attraction.

The used WFs included water as the reference and different concentrations of MNFs composed of a water solvent and magnetic nanoparticles of  $\text{Fe}_3\text{O}_4$  (Taiwan Advanced Nanotech Corp., Taoyuan, Taiwan). The crystallines of magnetic particles were analyzed, as shown in Figure 2a, using a powder X-ray diffractometer (D-500, Siemens Corp., Belgium, Germany) with  $\text{Cu-K}\alpha$  radiation at a wavelength of 0.15418 nm. Figure 2a shows that the phases of  $\text{Fe}_3\text{O}_4$  agreed with the standard diffraction spectrum (JCPDS no. 65–3107).

The size distribution of the magnetic particles was investigated, as shown in Figure 2b, using dynamic laser scattering (Nanotrac 150, Microtrac Corp., PA, USA). The average hydrodynamic diameter was  $10 \text{ nm} \pm 14 \text{ nm}$ . The diameter that was detected using dynamic laser scattering is a hydrodynamic diameter because detecting the Brownian motion of the particles was conducted by probing the Doppler frequency shift of the scattered light with respect to the incident light.

The magnetization properties of MNFs were examined using a vibration sample magnetometer (Model 4500, EG&G Corp, California, USA). The concentration of MNFs was diluted with deionized (DI) water. For example, the magnetization of 4 emu/g, equal to 0.8% in volumetric fraction, was obtained (Figure 2c).

#### Measurements and analysis models

In designing the decrease of the total thermal resistance ( $R_{WF}$ ) of an MNFHP, the major thermal resistance of the evaporator or condenser was reduced using MNFs with excellent thermal conductivity. The thermal resistance related with the MNF flowing between an evaporator and a condenser was accomplished by specifically configuring an MNFHP. Therefore, the improvement of the heat transfer in an evaporator or a condenser with magnetic fields was initially evaluated by testing the evaporator or condenser.

Both the evaporator and condenser were composed of a copper tube and a porous iron nozzle, as shown in the inset of Figure 3a,b. By connecting the stuffing parts, such as the charging valve and pressure gauge, the evaporator or the condenser was filled with the same amount of WFs. By setting the temperature of the heating or cooling sources ( $T_s$ ), the temperature variation of WFs,  $T_{WF}$ , was measured within different magnetic fields, for example, Figure 3a,b for the MNF of 0.8% in volumetric fraction. In addition, the heat transfer ( $Q$ ) contributed to WFs in two types: latent heat ( $Q_{\text{latent}}$ ) and sensible heat ( $Q_{\text{sensible}}$ ).  $Q_{\text{latent}}$  was the same regardless of whether the WFs were MNFs or water, but  $Q_{\text{sensible}}$  was the key property for distinguishing MNFs from water in thermal performance. Therefore,  $Q_{\text{sensible}}$  is representatively discussed using a one-dimensional model ( $Q_{\text{sensible}} = k_{WF}A_{WF} \frac{(T_{\text{tube}} - T_{WF})}{d_{WF}} = \rho_{WF}V_{WF}C_{WF} \frac{dT_{WF}}{dt}$ ). Here,  $Q_{\text{sensible}}$  is related to the thermal conductivity ( $k_{WF}$ ), temperature ( $T_{WF}$ ), density ( $\rho_{WF}$ ),

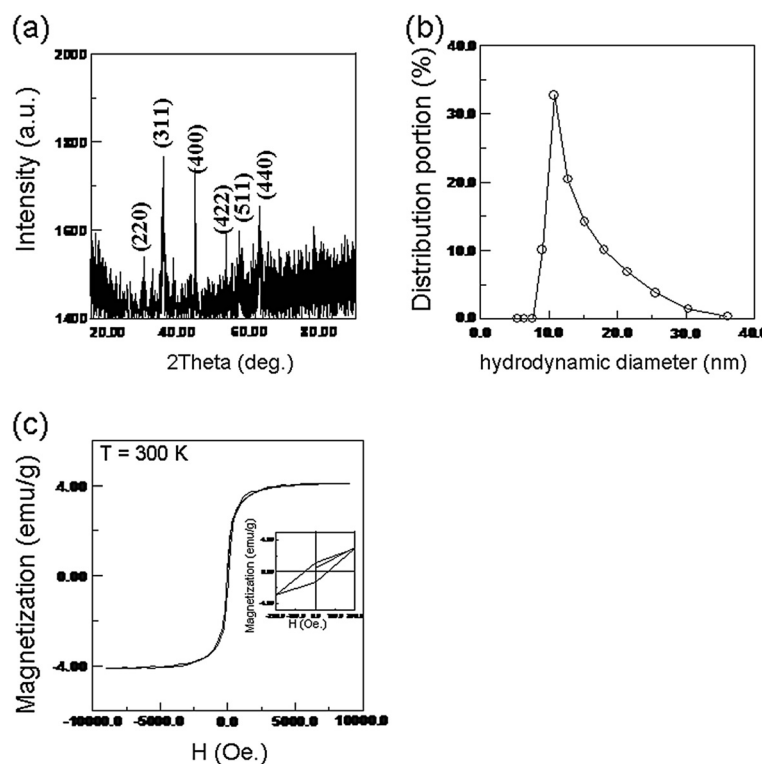


**Figure 2 Characterization of MNFs.** (a) The crystallines of magnetic nanoparticles, (b) hydrodynamic diameters of the magnetic nanoparticles, and (c) the magnetization properties.

specific heat ( $C_{WF}$ ), thickness ( $d_{WF}$ ), volume ( $V_{WF}$ ), cross-area ( $A_{WF}$ ) of the WFs between the outer surface of the iron nozzle and the inner surface of the evaporator or the condenser, and the tube temperature ( $T_{tube}$ ).  $T_{tube}$  is the same as  $T_s$  with the reasonable assumption of low thermal resistance, and  $t$  is the time after applying  $Q$ .

This one-dimensional model can be solved as  $T_{WF}$   

$$(T_{WF} = (T_{WF,0} - T_{tube})e^{-(k_{WF}A_{WF}/d_{WF}\rho_{WF}V_{WF}C_{WF})t} + T_{tube})$$
 from the initial temperature of the WFs ( $T_{WF,0}$ ). Here, the time constant ( $\tau$ ) of  $T_{WF}$  is the reciprocal of  $k_{WF}A_{WF}/d_{WF}\rho_{WF}V_{WF}C_{WF}$ . Furthermore,  $\tau$  is obtained according to the fitting of the  $T_{WF}$  variation with time, as shown in Figure 3a,b. To examine the influences of WFs and applied magnetic field ( $H$ ) on the conductivity of an evaporator or a condenser, the thermal indicator of  $k_{WF}/C_{WF}$  was analyzed based on  $T_{WF}$  under the reasonable assumption of the similar densities for water and MNFs for the test concentration of 0.8% and 0.003% in volumetric fraction. Hence, the enhanced ratio of  $k_{WF}/C_{WF}$  was defined as  $k_{MNF}C_w/k_wC_{MNF}$  to examine the effect of WFs by comparing  $C_{WF}$  and  $k_w$  of DI water.

Consequently, to determine the total thermal performance of the entire MNFHP, the proposed scheme was modified with some additional parts to measure the pressure and temperature, as well as the WF stuffing

(Figure 1). For different WFs or applied fields, the operation conditions were the same. In addition to the observation of the flowing pattern through the acrylic tube between the evaporator and condenser, the  $R_{WF}$  of the MNFHP, defined as  $(T_{evap} - T_{cond})/P$ , was analyzed. Here,  $T_{evap}$  and  $T_{cond}$  are the temperatures of WF in the evaporator and condenser, and the heat transfer of the heat pipes,  $P$ , is obtained via the thermal exchange of the cooling water surrounding the condenser. Similarly, the enhanced thermal resistance ratio ( $R_{MNF}/R_w$ ) was used to compare the effect of WFs, where  $R_{MNF}$  and  $R_w$  were under the MNFHP filled with MNFs and water, respectively.

## Results and discussion

Regarding the analysis of the thermal properties of an evaporator or a condenser, Figure 3a,b shows that  $T_{WF}$  increased or decreased exponentially over time for WFs of water or MNFs at different fields. For MNFs, both  $|T_{WF,f} - T_{tube}|$  and  $\tau$  decreased with  $H_s$  to optimal values at  $H$  of 200 Oe, where  $T_{WF,f}$  was the final temperature of WF. Furthermore, both  $|T_{WF,f} - T_{tube}|$  and  $\tau$  of MNFs were smaller than those of water. Based on the one-dimensional model,  $|T_{WF,f} - T_{tube}|$  decreased with the increase of  $k_{WF}$  under the same final heat

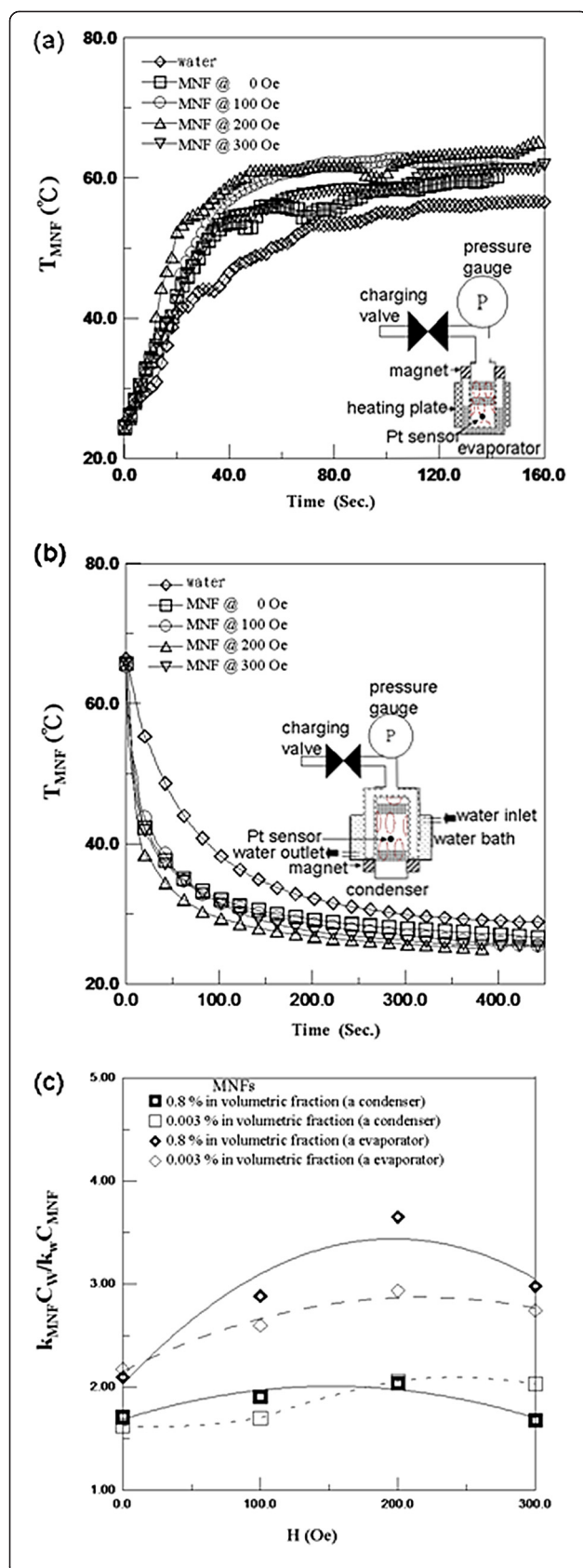


**Figure 3 Characterization of the subunit.** (a) The evaporator in the heating  $Q_{\text{sensible}}$  procedure, (b) the condenser in the cooling  $Q_{\text{sensible}}$  procedure, and (c) with the  $H$ -dependent  $k_{MNF} C_W / k_W C_{MNF}$ .

transfer,  $Q_{\text{sensible},f}$ , because  $Q_{\text{sensible},f}$  is equal to the system of heat loss. In addition,  $\tau$  could be evaluated according to the dominator of  $C_{WF} / k_{WF}$ . Therefore, the variations of  $|T_{WF,f} - T_{\text{tube}}|$  and  $\tau$  were related to the thermal parameters of  $k_{WF}$  and  $C_{WF}$ .

Furthermore, considering the variation of  $H_s$  and MNF concentrations in both the evaporator and condenser, Figure 3c indicates that all  $k_{MNF} C_W / k_W C_{MNF}$  increased with  $H_s$  and have an optimal value at a specific  $H$ . The optimal phenomenon was not significant for low concentrations of MNFs. Moreover, the  $k_{MNF} C_W / k_W C_{MNF}$  of the evaporator was larger than that of the condenser. The reasons were explained in  $k_{WF}$  and  $C_{WF}$  at different  $H_s$  and temperatures.

For magnetic nanoparticles of  $\text{Fe}_3\text{O}_4$ ,  $k_{MNF}$  was larger than  $k_W$  in proportion to the concentration [8,9].  $k_{MNF}$  increased with  $H_s$  and had an optimal value at a specific  $H$  [8,9]. The specific field increased, whereas the concentration was lower [8]. Because of the formation of magnetic clusters,  $C_{MNF}$  decreased with  $H_s$ , becoming smaller than 300 Oe [14]. Because the origin of mechanism is the same as that of  $k_{MNE}$  there was possibly an optimal value for the variation of  $C_{MNF}$  with  $H_s$ . This was valid for other  $H$ -dependent optical properties of MNFs based on this mechanism [15]. Regardless,  $k_{MNF} / C_{MNF}$  had an optimal value at a specific  $H$ , but  $k_W / C_W$  maintained the same value for all  $H_s$ .

In WF temperature,  $k_{MNF}$  decreased as the temperature rose [16], but  $k_W$  almost remained the same [17]. Similarly,  $C_{MNF}$  decreased slightly as the temperature rose, but  $C_W$  almost remained the same [14]. Effectively,  $k_{MNF} C_W / k_W C_{MNF}$  is smaller at high temperatures than at low temperatures if the effect of  $C_{MNF}$  is smaller than that of  $k_{MNF}$ .

Therefore, for the enhanced time of heat transfer in an evaporator or a condenser,  $k_{MNF} C_W / k_W C_{MNF}$  as depicted in Figure 3c, achieved up to 3.5 and 1.6, separately, under the optimal condition of MNFs of 0.8% in volumetric fraction at 200 Oe.

Furthermore, by filling MNFs with 0.8% in volumetric fraction into an entire MNFHP, thermal performance of  $R_{MNF} / R_W$  at different  $H_s$  was analyzed in Figure 4a, indicating that  $R_{MNF} / R_W$  was less than 1 at all  $H_s$  except zero field. The worst  $R_{MNF}$  at zero fields was unexpected according to  $k_{MNF} C_W / k_W C_{MNF}$  of a single evaporator or a condenser in the  $Q_{\text{sensible}}$  test, larger than 1. Possibly, MNF with the high concentration easily resulted in the deposition of magnetic nanoparticles on the tube

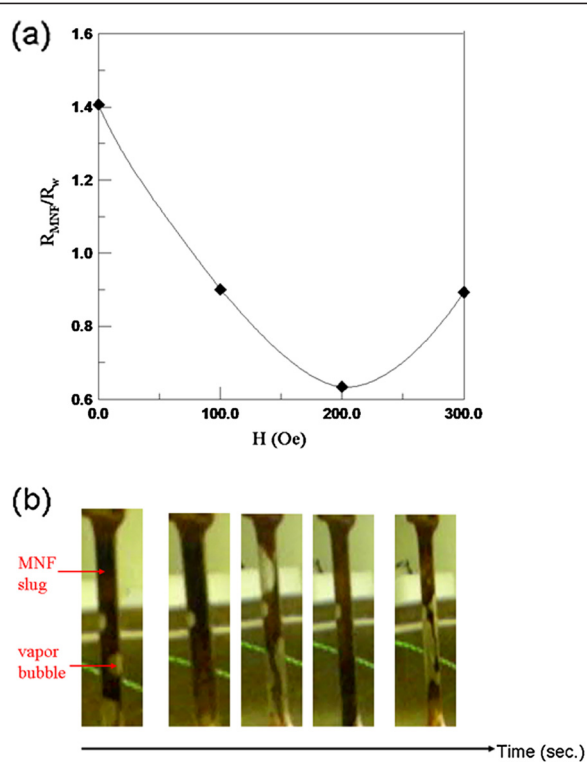


**Figure 4 Characterization of a MNFHP filled with MNFs of 0.8% in volumetric fraction. (a)** The  $H$ -dependent  $R_{\text{MNF}} / R_W$ , and **(b)** the flowing pattern at 200 Oe.

wall of the evaporator. Conversely, for the smaller  $R_{\text{MNF}} / R_W$  at the nonzero field, the deposition phenomenon was possibly avoided. The reason was that the more violent scour on the tube walls of a condenser and an evaporator caused by the faster MNF flowing under higher  $k_{\text{MNF}}C_W / k_W C_{\text{MNF}}$  might decrease the MNP deposition. The minimum of  $R_{\text{MNF}} / R_W$  occurred at the same as 200 Oe with  $k_{\text{MNF}}C_W / k_W C_{\text{MNF}}$  of a single evaporator and condenser in Figure 3c. Furthermore,  $R_{\text{MNF}} / R_W$  of the entire MNFHP could be viewed as the ratio of the effective thermal conductivity ( $k_{W,\text{MNFHP}} / k_{MNF,\text{MNFHP}}$ ) with a simple conduction model in that the thermal resistance  $R$  was equal to  $k_{WE,\text{MNFHP}} A_{\text{tube}} / d_{\text{tube}}$ , where the effective thermal conductivity of the entire MNFHP filled with some WF ( $k_{WE,\text{MNFHP}}$ ), the cross area ( $A_{\text{tube}}$ ) and diameter ( $d_{\text{tube}}$ ) of the tube are in form, derived from the one-dimensional conduction model. Therefore, the minimal value of  $R_{\text{MNF}} / R_W$  of approximately 0.6 was equal to this maximal value of  $k_{MNF,\text{MNFHP}} / k_{W,\text{MNFHP}}$  of 1.6. This value is similar with the smaller optimal value of  $k_{\text{MNF}}C_W / k_W C_{\text{MNF}}$  in a single condenser rather than that of the larger single evaporator. It could be concluded that the thermal performance of an entire MNFHP was limited by the smaller one because of the

series assembly of an evaporator and a condenser, as well as a minor thermal resistance of the flowing mechanism.

Moreover, under the optimal condition of MNFs of 0.8% in volumetric fraction at 200 Oe, the total thermal performance of the entire MNFHP under the optimal condition achieved the maximal  $P$  of 60 W and the flowing pattern of the MNF slug and vapor bubble, as shown in the photos at the time interval of 1 sec in Figure 4b, was observed in the acrylic tube between the evaporator and the condenser, thus confirming that the flowing pattern was the design.

## Conclusion

This study developed an MNFHP in a closed-loop scheme with magnetically enhanced thermal properties, the flowing pattern of the interval liquid slug and vapor bubble, and the separated paths of evaporated fluids and condensed fluids. The feasibility of an MNFHP with magnetically enhanced thermal performance is valid. The enhanced thermal conductivity ratio of an MNFHP showed that the entire MNFHP was limited by the  $k_{\text{MNF}}C_W / k_W C_{\text{MNF}}$  of a condenser subunit. This was useful in designing an MNFHP.

## Abbreviations

DI: deionized; MNFs: magnetic nanofluids; MNFHP: magnetic-nanofluid heat pipe; WFs: working fluids.

## Competing interests

The authors declare that they have no competing interests.

## Authors' contributions

YCC conducted the experiment. JJC provided the idea and proofread the manuscript. CCH provided technical support for the manufacturing equipment. All authors read and approved the final manuscript.

## Authors' information

YCC has been an assistant professor in the Department of Mechanical Engineering, Chinese Culture University. His research interests include thermodynamics, heat transfer in electronics, and energy engineering. JJC has been an associate professor in the Institute of Electro-Optical Science and Technology, National Taiwan Normal University. His research interests include photonics, energy, and biomagnetism. CCH was a PhD degree candidate in the Department of Mechanical Engineering, National Central University. He had rich practical experiences of related manufacturing equipment in addition to his major in micro- and nano-scale manufacturing.

## Acknowledgment

The financial support of this work was provided by the National Science Council, Taiwan, under grant number NSC98-2622-E003-003-CC3.

## Author details

<sup>1</sup>Department of Mechanical Engineering, Chinese Culture University, No. 55, Hwa-Kang Rd., Yang-Ming-Shan, Taipei 111, Taiwan. <sup>2</sup>Institute of Electro-Optical Science and Technology, National Taiwan Normal University, No.88, Sec.4, Ting-Chou Rd., Taipei 116, Taiwan. <sup>3</sup>Department of Mechanical Engineering, National Central University, No.300, Jhongda Rd., Jhongli City, Taoyuan County 32001, Taiwan.

Received: 12 May 2012 Accepted: 10 June 2012

Published: 20 June 2012

## References

1. Wang XQ, Mujumdar AS: Heat transfer characteristics of nanofluids: a review. *Int J Therm Sci* 2007, **46**:1–19.
2. Kang SW, Wei WC, Tsai SH, Huang CC: Experimental investigation of nanofluids on sintered heat pipe thermal performance. *Appl Therm Eng* 2009, **29**:973–979.
3. Tsai CY, Chien HT, Ding PP, Chan B, Luh TY, Chen PH: Effect of structural character of gold nanoparticles in nanofluid on heat pipe thermal performance. *Mat Lett* 2004, **58**:1461–1465.
4. Ma HB, Wilson C, Borgmeyer B, Park K, Yu Q, Choi SUS, Tirumala M: Effect of nanofluid on the heat transport capability in an oscillating heat pipe. *Appl Phys Lett* 2006, **88**:143116-1-143116-3.
5. Charoensawan P, Khandekar S, Groll M, Terdtoon P: Closed loop pulsating heat pipes part a: parametric experimental investigations. *Appl Therm Eng* 2003, **23**:2009–2020.
6. Charoensawan P, Khandekar S, Groll M, Terdtoon P: Closed loop pulsating heat pipes part b: visualization and semi-empirical modeling. *Appl Therm Eng* 2003, **23**:2021–2033.
7. Mehta RC, Jayachandran T: Numerical analysis of transient two phase flow in heat pipe. *Heat Mass Transfer* 1996, **31**:383–386.
8. Philip J, Shima PD, Raj B: Enhancement of thermal conductivity in magnetite based nanofluid due to chainlike structures. *Appl Phys Lett* 2007, **91**:203108-1-203108-3.
9. Philip J, Shima PD, Raj B: Nanofluid with tunable thermal properties. *Appl Phys Lett* 2008, **92**:043108-1-043108-3.
10. Yang XF, Liu ZH, Zhao J: Heat transfer performance of a horizontal micro-grooved heat pipe using CuO nanofluid. *J Micromech Microeng* 2008, **18**:035038-1-035038-6.
11. Huang WZ: Heat pipe, PRC patent; 2008. CN 100425935C.
12. Zhang M, Liu ZL, Ma GY, Cheng SY: The experimental study on flat plate heat pipe of magnetic working fluid. *Exp Therm Fluid Sci* 2009, **33**:1100–1105.
13. Chieh JJ, Lin SJ, Chen SL: Thermal performance of cold storage in thermal battery for air conditioning. *Int J Refrig* 2004, **27**:120–128.
14. Chiu YP, Chen YF, Yang SY, Chen JC, Horng HE, Yang HC, Tse WS, Hong CY: Specific heat of magnetic fluids under a modulated magnetic field. *J Appl Phys* 2003, **93**:2079–2081.
15. Chieh JJ, Yang SY, Horng HE, Hong CY, Yang HC: Magnetic-fluid optical-fiber modulators via magnetic modulation. *Appl Phys Lett* 2007, **90**:133505-1-133505-3.
16. Safonenko AGR, Volkova NE: Specific features of temperature dependence of the thermal conductivity of water-based magnetic fluids. *J Magn Magn Mater* 1993, **122**:19–23.
17. Li CH, Peterson GP: Experimental investigation of temperature and volume fraction variations on the effective thermal conductivity of nanoparticle suspensions (nanofluids). *J Appl Phys* 2006, **99**:084314-1-084314-8.

doi:10.1186/1556-276X-7-322

**Cite this article as:** Chiang et al.: The magnetic-nanofluid heat pipe with superior thermal properties through magnetic enhancement. *Nanoscale Research Letters* 2012 **7**:322.

Submit your manuscript to a SpringerOpen® journal and benefit from:

- Convenient online submission
- Rigorous peer review
- Immediate publication on acceptance
- Open access: articles freely available online
- High visibility within the field
- Retaining the copyright to your article

Submit your next manuscript at ► [springeropen.com](http://springeropen.com)